ACS OMEGA

Open Access

http://pubs.acs.org/journal/acsodf

Article

Study on the Enhanced Oil Recovery Properties of the Pickering Emulsions for Harsh Reservoirs

Liu Yang, Jijiang Ge, Hao Wu, Xiaqing Li, Jianda Li, and Guicai Zhang*

Cite This: *ACS Omega* 2024, 9, 48427−48437

Read Online

ACCESS | Metrics & More | Article Recommendations

ABSTRACT: Pickering emulsions stabilized by surfactant-modified SiO_2 nanoparticles demonstrate good stability against droplet coalescence, showing application potential for enhanced oil recovery in high-temperature and high-salinity environments. Adjusting the adsorption ratio of surfactant on the nanoparticles significantly affects the wettability of nanoparticles and therefore regulates the microstructure and properties of Pickering emulsions. In this study, a saturated monolayer adsorption occurs at a surfactant-to-nanoparticles ratio of 0.1:1.0%, where an optimal hydrophilic−hydrophobic balance is achieved. However, below or above this ratio, the SiO_2 nanoparticles become more hydrophilic with the decreasing or increasing surfactant concentration. Pickering emulsions stabilized by the intermediate wet nanoparticles exhibit the best stability and highest viscosity. Laser confocal scanning microscopy and cryo-scanning electron microscopy reveal that the SiO_2 nanoparticles can form a bridge-structure network among the droplets of these emulsions. Microfluidic experiments and sand pack experiments show that Pickering emulsions provide greater permeation resistance than conventional emulsions stabilized solely by surfactant solely. In addition, microscopic experiments show that Pickering emulsions enhance oil recovery by 20% after second waterflooding, compared to a 12% recovery rate with conventional emulsions. It is found that the Pickering emulsions with bridge-structures may be accumulated in and plug channels much larger than their droplets, which results in higher properties of conformance control.

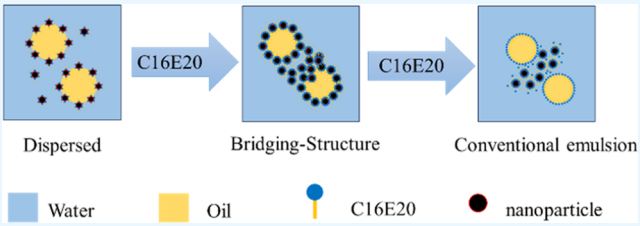

1. INTRODUCTION

Emulsions are mixtures of immiscible or slightly miscible liquid phases where one liquid is dispersed as droplets within another continuous liquid phase. Typically involving an aqueous phase and an oil phase, emulsions are thermodynamically unstable due to the large interface between the two phases. This instability can lead to issues such as creaming, sedimentation, coalescence, and Ostwald ripening.[1−3] In many applications, such as enhanced oil recovery (EOR) in oilfields,[4] stable emulsions are essential. However, conventional emulsions stabilized by surfactants or polymers often fail under harsh reservoir conditions, such as high temperatures and high salinity. To address these challenges, recent research works have focused on using nanoparticles to improve emulsion stability.[5−7] These advancements have shown promise in enhancing the properties of emulsions, potentially broadening their applications in the oilfield.

No more one-third of the original oil in place (OOIP) can be recovered through primary and secondary methods, which depend on natural reservoir energy and waterflooding, respectively.[8] To enhance oil production, various EOR methods, such as thermal recovery,[9,10] miscible flooding,[11] and chemical flooding,[12,13] have been employed in oilfield development. Among these, chemical flooding has yielded notable results over the past two decades, such as Pelican Lake oilfield in Canada and Daqing oilfield in China.[14,15] Chemical flooding involves injecting chemicals such as surfactants, polymers, alkaline substances, and their combinations into the reservoir to recover more oil after waterflooding. This method enhances oil recovery by altering wettability, reducing interfacial tension (IFT), and improving the mobility ratio, potentially increasing recovery by 10−20%.[16−18] The formation of emulsions has been shown to be crucial in this process.[19,20] Laboratory experiments indicate that oil recovery can decrease by 5% if no emulsions were formed during chemical flooding.[21] For example, emulsions can be formed between crude oil and water in the presence of surfactants or polymers during chemical flooding. These emulsions improve displacement efficiency through the emulsification and carrying mechanisms.[22,23] More importantly, they can increase the sweep efficiency by plugging water channels. As emulsion droplets pass through pore throats, they deform and create additional capillary pressure differences, known as the Jamin effect.[24] This resistance to water flow

Received: July 25, 2024
Revised: November 14, 2024
Accepted: November 15, 2024
Published: November 26, 2024

redirects the aqueous phase to oil-rich, low-permeability zones. In some instances, emulsions are prepared on the ground and injected into the system as oil displacement agents. However, the mentioned chemical flooding methods face significant challenges in high-temperature and high-salinity reservoirs. For example, the viscosity of polymer solutions decreases dramatically with increasing temperature and salinity, directly reducing their effectiveness in mobility control. Consequently, polymer flooding is typically limited to reservoirs below 70 °C.[25,26] Although many temperature- and salt-resistant surfactants have been developed in recent years, using a single surfactant solution without polymers remains less effective for EOR due to its poor water-to-oil mobility ratio. Additionally, the harsh reservoir conditions also reduce the stability of the emulsions, manifested as droplet coalescence, which limits their effectiveness in tertiary oil recovery.

Recent advancements have been made by adding nanoparticles to improve emulsion stability, expanding the application limit of emulsions.[27,28] In 1903, Ramsden found that solid particles can stabilize emulsions, and subsequently, Pickering conducted a more systematic study in 1907. It was discovered that solid particles, when possessing the appropriate wettability, can adsorb at the oil/water interface and stabilize emulsion droplets. Emulsions stabilized by solid particles are known as Pickering emulsions. The stability of these emulsions is heavily dependent on the adsorption of particles at the oil−water interface. The desorption energy of spherical particles at the oil−water interface can be expressed as

$$E = \pi r^2 \gamma (1 - \cos\theta)^2 \quad (1)$$

Here, E represents the energy required for a single particle to detach from the oil−water interface into the water phase, typically measured in units of k_BT[29−31] (where k_B is Boltzmann's constant, 1.38×10^{-23} J/K; and T is the absolute temperature in Kelvin). Besides, r is the radius of the particles in nanometers, γ is the oil−water interfacial tension in mN/m, and θ is the three-phase contact angle between oil, water, and solid at the surface of the particle. Typically, the desorption energy of these particles ranges from hundreds to thousands of k_BT, significantly higher than the desorption energy of surfactant molecules, which is usually a few k_BT. Consequently, Pickering emulsions are much more stable against coalescence than conventional emulsions. Various solid particles can fulfill this role by meeting three key requirements: (a) being significantly smaller than the droplet size, (b) being partially wetted by both oil and water phases, and (c) exhibiting a degree of particle flocculation. Recently, there has been increasing interest in nanoparticles as stabilizers for Pickering emulsions, driven largely by their ability to tailor hydrophilic and hydrophobic properties with ease. Various nanoparticles are reported to prepare Pickering emulsions, including nano-SiO_2, nano-Al_2O_3, nano-TiO_2, montmorillonite, and lithium saponite.[32−36] Besides, organic particles,[7,37−40] such as polystyrene microspheres, nanocellulose, protein microspheres, and graphene oxide, are also reported. Binks et al.[41−43] have investigated the preparation and stability mechanism of Pickering emulsions stabilized by surfactant-modified SiO_2 nanoparticles. The natural SiO_2 nanoparticles are strongly hydrophilic and exhibit weak interfacial activity so that they should be wetting modified by mixing with a nonionic surfactant or cationic surfactant. These surfactants adhere to the nanoparticles surface through hydrogen bonding or electrostatic interactions, rendering the nanoparticles moderately wettable and capable of adsorbing at the oil−water interface. Beside of the adsorption mechanism, the electrostatic repulsion between the nanoparticles and the surfactant is found to be benefit for emulsion stability. Recently, Xu et al.[44,45] introduced a novel approach to stabilize emulsions by using nanoparticles with the same charge as the surfactant. They prepared *n*-decane-in-water emulsions using the cationic surfactant hexadecyltrimethylammonium bromide (CTAB) as the emulsifier. It was observed that a surfactant concentration of >0.6 mmol/L was necessary to stabilize the emulsion. However, upon adding 0.5 wt % Al_2O_3 nanoparticles, which are also positively charged, the critical surfactant concentration was significantly reduced from 0.1 mmol/L to 0.001 mmol/L, resulting in stable emulsions that remained intact for over a month. Further experiments indicated that the Al_2O_3 nanoparticles predominantly dispersed in the aqueous phase, where they prevented the emulsion droplets from coalescing through electrostatic repulsion. However, the stability of these electrostatically stabilized emulsions in response to salinity and its potential chromatographic separation in the reservoir has not yet been validated.

Overall, Pickering emulsions have shown excellent potential for EOR in an oilfield. The main advantage is their high efficiency in preventing droplets from coalescence under harsh reservoir conditions. Midmore[46] found that stable emulsions could be obtained even the coverage rate of the SiO_2 nanoparticles on the oil−water interface was 29%. In Vignati's study,[47] the coverage rate was only 5%. Maurya[48] prepared Pickering emulsions that could endure the temperature of 90 °C, which is satisfied for most chemical flooding in oilfield. Murray[49] investigated the effect of electrolyte on the stability of Pickering emulsions and found that the addition of NaCl improved the hydrophobicity of nanoparticles. In other words, the in situ modification of the surfactant on the nanoparticles is enhanced at higher salinity. Besides their stability, Pickering emulsions exhibit excellent rheological properties,[50,51] including high viscosity and thixotropy, which are beneficial for conformance control applications.

However, the application limit of Pickering emulsions in an oilfield is still not clear. Referring to the EOR mechanism of Pickering emulsions, most of the previous studies contributed to their high viscosity, but the effect of the unique microstructure of Pickering emulsions was ignored. This work explores their suitability for oilfield applications through experiments focused on system preparation, stabilization mechanisms, and rheological properties. In particular, the effectiveness of Pickering emulsions for EOR is examined across a visually microscopic model.

2. MATERIALS AND METHODS

2.1. Materials. Colloidal SiO_2 (Ludox SM-30) was procured from Sigma-Aldrich at a concentration of 30%. The nanoparticles exhibited a specific surface area of 220 m^2/g and a manufacturer-reported pH of 12. The size of nanoparticles was characterized by dynamic light scattering using Malvern Nano-ZS90 (Malvern Company, England). It was measured that the median diameter of the nanoparticles was 14 nm and the size distribution ranged from 6 to 30 nm. The isoelectric point of the nanoparticles was measured to be approximately pH = 2.3. A nonionic surfactant, cetyl polyoxyethylene ether (20) (C16E20), was obtained from Alfa Aesar and was of analytical purity. The chemical formula of C16E20 is $C_{16}H_{33}(OCH_2CH_2)_{20}OH$, and its structure is displayed in Figure 1. The surfactant C16E20 is a white solid with a molecular weight of 545.49 g/mol. Prior to experiments, the

https://doi.org/10.1021/acsomega.4c06834
ACS Omega 2024, 9, 48427−48437

Figure 1. Chemical formula of C16E20.

critical micelle concentration of C16E20 was measured to be 5×10^{-3} wt %, obtained from its surface tension curve. Besides, 1% C16E20 solutions were found to be transparent at 120 °C, indicating that its cloud point is high enough for EOR. Liquid paraffin, sourced from Acros, was used as the oil phase in the emulsions. Before use, the liquid paraffin underwent purification by being passed through an alumina column three times to remove dissolved polar substances. Hydrochloric acid (HCl) and sodium chloride (NaCl), purchased from Sinopharm Chemical Reagent and meeting analytical purity standards, were employed for pH adjustment and to control the salinity of the solutions and emulsions during the experiments.

2.2. Measurement of Contact Angle. The contact angle of a captive paraffin oil drop in 0.1% C16E20 solutions on a SiO_2-based quartz was measured by Drop Shape Analyzer 100 (Kruss, Germany). First, the quartz was immersed in the C16E20 solution for 12 h. Second, the oil drop was added under the quartz. Third, the value of the contact angle was obtained from the software.

2.3. Preparation of Emulsions. The majority of the emulsions in our study were prepared using a 1% NaCl solution. Initially, a solution containing a surfactant and nanoparticles was prepared. The concentration of C16E20 ranged from 0.001 to 1.0%, while the concentration of SiO_2 nanoparticles was fixed at 1.0%. Subsequently, the pH of these solutions was adjusted to 6 using a diluted HCl solution. We observed that the adsorption efficiency of C16E20 on SiO_2 nanoparticles decreased with increasing pH. At pH $\leq$ 6, the adsorption efficiency was as high as 98%.[41] Therefore, all of the emulsions were prepared at pH 6. To prepare the emulsions, 6 mL of liquid paraffin and 24 mL of the above-prepared mixture (resulting in an oil−water volumetric ratio of 1:4) were combined in sample vials and stirred for 2 min at 15,000 rpm using a T18 high-speed homogenizer (IKA, Germany). The resulting emulsions were then placed in an oven and aged at 80 °C.

2.4. Stability of Emulsions. Emulsion stability was assessed using the released oil fraction (ROF) and droplet radius change (DRC), calculated as follows:

$$\mathrm{ROF} = \frac{V_r}{V_t} \times 100\% \tag{2}$$

$$\mathrm{DRC} = \frac{R}{R_0} \tag{3}$$

where ROF refers to the ratio of the released oil to the total oil, %; V_r is the volume of the released oil phase, mL, obtained by visual inspection method; V_t is the total volume of the oil phase in the emulsion, mL; DRC is the ratio of the droplets radius to the initial average radius; R is the average radius of the emulsion droplets, μm; R_0 is the initial average radius of the emulsion droplets, μm, and it was measured in 10 min after preparation of the emulsions. The average radius of the emulsions was measured by an OLYMPUS CX33 microscope (Olympus company, Japan). The measurements of ROF and DRC were repeated three times, and the error bars are listed in the figures.

2.5. Microstructure of Emulsions. The emulsion's microstructure was examined using confocal laser scanning microscopy (CLSM) and cryo-scanning electron microscopy (cryo-SEM). For CLSM analysis, nanoparticles were fluorescently labeled with a 10^{-5} mol/L Rhodamine B solution prior to emulsion preparation. Before the experiments, the emulsion samples were diluted by distilled water. Imaging was conducted using a Fluo ViewTM FV1000 system (Olympus company, Japan), with the CLSM laser operating at a 560 nm wavelength to induce red fluorescence from Rhodamine B under laser irradiation. Cryo-SEM observations were performed using a Hitachi Regulus 8220 (Hitachi company, Japan). Initially, samples were rapidly frozen under vacuum conditions at −100 °C for 2 min and then fractured. The temperature was subsequently reduced to −120 °C, and a thin layer of 2 nm platinum particles was deposited on the fractured samples. Finally, the samples were imaged under SEM at an accelerating voltage of 3.0 kV to examine their detailed microstructure.

2.6. Rheology of Emulsions. Rheological experiments on the emulsions were performed using an Anton Paar MCR 92 rheometer (Anton Paar Company, Austria). The viscosity of the emulsions was measured by using a CP39 coaxial cylinder. The shear rate was varied logarithmically from 1 to 100 s^{-1}, with a total of 25 data points taken and a shear time of 20 s for each point.

2.7. EOR Properties of Emulsions. EOR properties of the Pickering emulsions were characterized through three flow models, including the microfluidics model, the sand pack model, and the visual two-dimensional (2D) model. Thus, the migration and retention properties of the emulsion droplets, the conformance control of the emulsions, and the oil displacement properties of the emulsions were investigated, respectively. The parameters of the models and the experimental details were introduced as follow:

The structure of the microfluidics model is illustrated in Figure 2. The oil and water phases were injected into the model

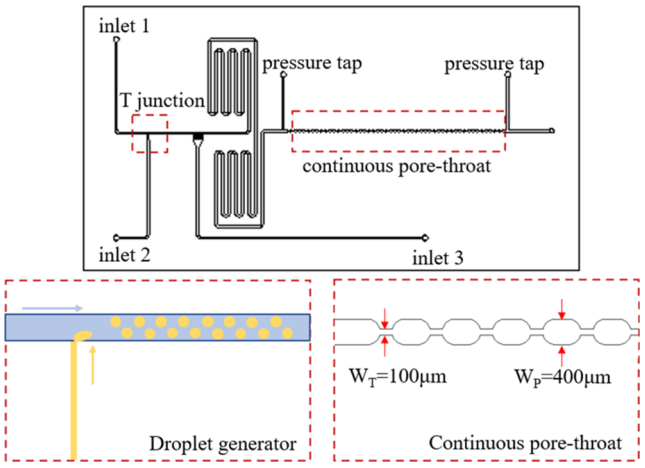

Figure 2. Structural diagram of a continuous pore-throat micromodel.

by an injection pump through inlets 1 and 2, respectively. The T-zone was a droplets generator, where the nonwetting oil phase was sheared into droplets by the wetting water phase, and emulsions was prepared. The parameters such as oil−water ratio and flow rate were adjusted through the injection rate of three inlets. Consequently, the droplet size can also be adjusted by the above parameters. The depth of each channel in this model was 100 μm. In a continuous pore-throat structure, the width of the main channel was 400 μm, and the width of the pore throat was 100 μm. AE2000 inverted microscope (Motic, China) was used

https://doi.org/10.1021/acsomega.4c06834
ACS Omega 2024, 9, 48427−48437

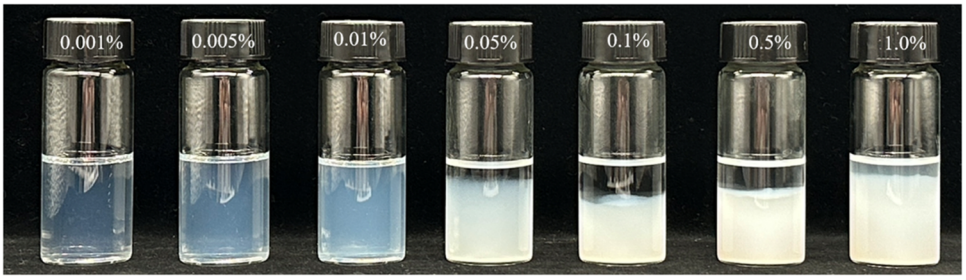

Figure 3. Dispersed state of 1% nanoparticles in 0.001−1.0% C16E20 solutions after aging for 12 h at room temperature.

to observe the migration and retention characteristics of emulsions in porous media under a double objective lens, and the pressure difference between the two ends of porous media was recorded.

Sand pack models with permeabilities of about 1000 mD were prepared in this study. The diameter and length of the sand packs were 2.0 and 10.0 cm, respectively. The sand packs were first saturated by injecting distilled water with resistivity of 18Ω at 0.1 mL/min. Thus, the permeability was determined from Darcy's equation, and the porosity was determined by the weight difference. Second, about 2 pore volumes (PV) of emulsions were injected into the sand pack at 0.1 mL/min. Finally, distilled water was injected again at a rate of 0.1 mL/min until the injected pressure became stable.

Oil displacement experiments were performed on a visual 2D model in size of 40 × 40 mm. The model was made of glass and relatively homogeneous porous medium etched in depth of about 40 μm. A crude oil with initial viscosity of 2.3×10^4 mPa·s was diluted by kerosene and was used as the simulated oil. The viscosity of the simulated oil was 83 mPa·s, and the mixture was filtered to remove solid particles before experiments. During the experiments, the simulated oil, water, and emulsions were successively injected into the model by an injection pump, with a flow of 0.05 mL/min. The total process of the experiments was recorded with a digital microscope.

3. RESULTS AND DISCUSSION

3.1. Interaction between Surfactant and Nanoparticles. Figure 3 illustrates the mixture solutions containing SiO_2 nanoparticles and a surfactant. The dispersion state of SiO_2 nanoparticles undergoes a process of dispersion, flocculation, and redispersion with increasing C16E20 concentration. At concentrations below 0.01%, the nanoparticles remain dispersed in the mixture solution. In a weakly acidic environment, the oxygen vinyl groups on C16E20 molecules may form hydrogen bonding with −Si−OH groups of the nanoparticles. Therefore, the surfactants are absorbed on the nanoparticles, exposing their alkyl chain on the surface of the nanoparticles.[29] Consequently, the wettability of the nanoparticles is shifted from hydrophilic to hydrophobic states with the C16E20 concentration. As the C16E20 concentration reaches 0.05%, significant flocculation can be observed. However, when the C16E20 concentration is higher than 0.1%, the flocculation is weakened with the C16E20 concentration, indicating that the hydrophilic property of the nanoparticles is increased.[41,44] As Binks et al.[42−44] reported, when the surfactant concentration exceeds the saturation amount for monolayer adsorption, the alkyl chains of the excess surfactant and the adsorbed ones may associate with each other via hydrophobic effect. As a result, the oxygen vinyl groups of the surfactant are exposed, and the nanoparticles become hydrophilic again.

To further prove the adsorption of surfactant on the nanoparticles, the contact angle is measured[49] with the concentration of C16E20, as showed in Figure 4. When the

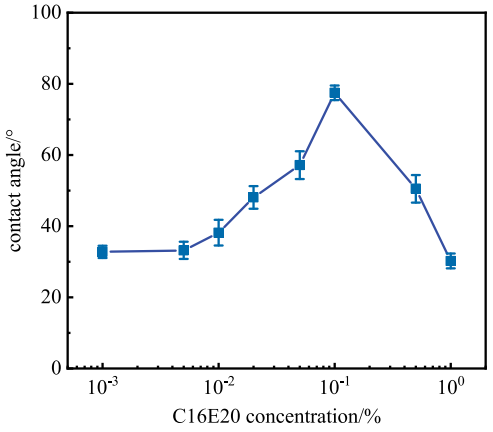

Figure 4. Contact angle of 1% nanoparticle solutions with C16E20 concentration ranging from 0.001 to 1.0%.

C16E20 concentration is lower than 0.005%, the contact angle is 32°, meaning that the SiO_2 nanoparticles are strongly hydrophilic. Subsequently, the contact angle is increased with the C16E20 concentration and reaches the maximum value 78° at 0.1% C16E20. It is indicated that the wettability of the nanoparticles is alerted from hydrophilic to near-neutral wetting. According to the mechanism of the formation of the Pickering emulsions, the near-neutral wettability is a benefit for the nanoparticles to adsorb on the oil−water interface. As the C16E20 concentration is higher than 0.1%, the contact angle is decreased and reaches 30° at 1.0% C16E20 concentration. In conclusion, the wettability of the SiO_2 nanoparticles may be adjusted by the adsorption the surfactant. During monolayer adsorption, the hydrophobicity of the nanoparticles is enhanced with the surfactant concentration.

Figure 5 illustrates both conventional emulsions stabilized by C16E20 and Pickering emulsions stabilized by modified SiO_2 nanoparticles, in which the emulsions are aged for 12 h at room temperature after preparation. Conventional emulsions stabilized solely by C16E20, ranging in concentration from 0.001 to 1.0%, exhibit stability without phase separation of the oil component. The emulsion volume remains consistent across surfactant concentrations, constituting approximately one-third of the total volume for all samples. In contrast, Pickering emulsions exhibit a distinct behavior dependent on surfactant concentration, similar to the nanoparticle dispersion observed in Figure 3. At C16E20 concentrations between 0.001 and 0.01%, the emulsions are predominantly found in the upper layer of the samples, with the lower layer consisting of aqueous phase. As

https://doi.org/10.1021/acsomega.4c06834
ACS Omega 2024, 9, 48427−48437

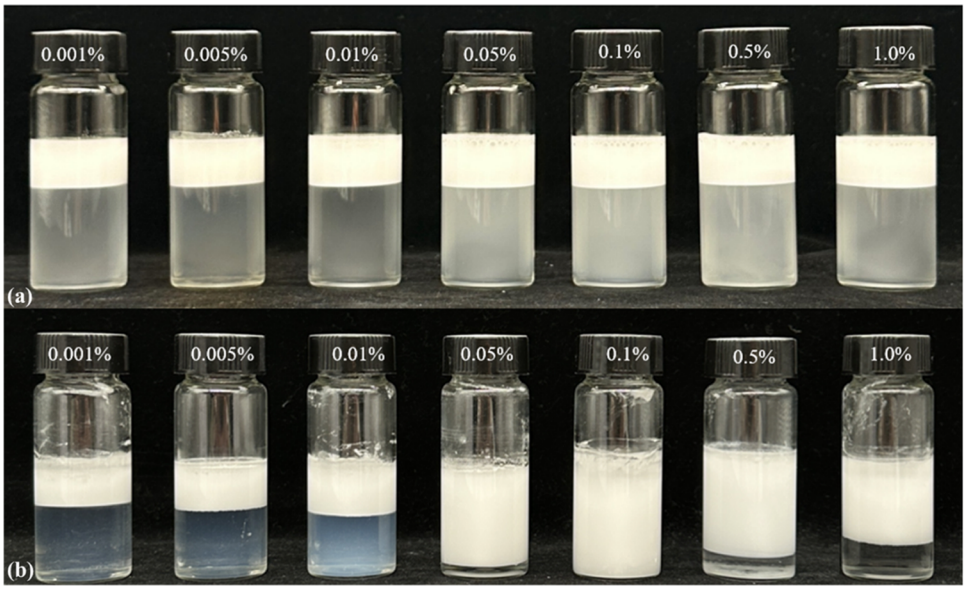

Figure 5. Emulsions stabilized by (a) 0.001−1.0% C16E20 alone and (b) 1.0% SiO_2 nanoparticles and 0.001−1.0% C16E20 after aging for 12 h at room temperature.

surfactant concentration increases, the volume of emulsions in the upper layer expands, while turbidity in the lower aqueous phase diminishes. This trend correlates directly with the nanoparticles' wettability: below the saturation adsorption of nanoparticles, a significant number of nanoparticles remain dispersed in the aqueous phase. At C16E20 concentrations between 0.05 and 0.1%, typical Pickering emulsions are observed where the emulsion volume dominates the liquid phase. However, further increases in C16E20 concentration lead to a gradual reduction in emulsion volume, accompanied by increased separation of water phase.

3.2. Stability and Rheology of Pickering Emulsions. Figure 6 presents the stability of Pickering emulsions under reservoir conditions, characterized by ROF and DRC. Unlike conventional emulsions, the stability of Pickering emulsions shows a nonlinear relationship with surfactant concentration. Initially, during the early aging stage (10 days), all emulsions exhibit stability with minimal oil phase coalescing, and the

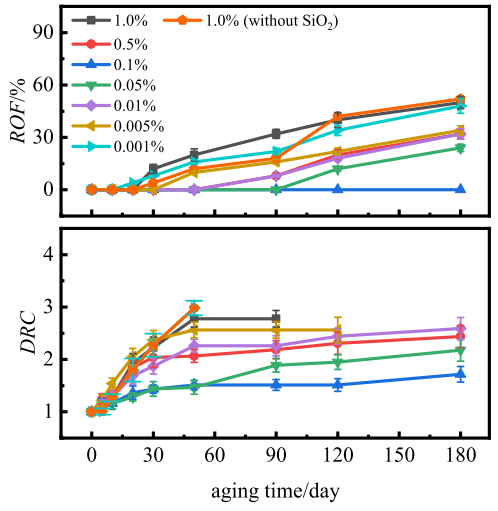

Figure 6. ROF and DRC of the emulsions with 0.001−1.0% C16E20 and 1.0% SiO_2 nanoparticles aging at 80 °C.

average droplet size increases by only 10% compared to fresh emulsions. However, with prolonged aging, emulsion stability varies significantly with the surfactant concentration. For instance, at a C16E20 concentration of 0.001%, the oil phase coalesced begins after approximately 20 days, reaching an ROF of 45% after 180 days. The DRC curve forms an S-shaped pattern, indicating initial droplet aggregation within the first 20 days, followed by a gradual increase in droplet size, which triples after 45 days. The lag observed in the ROF curves compared to the DRC curves suggests that the oil phase coalesced results from droplet aggregation and accumulation. In the C16E20 concentration range of 0.001−0.1%, increasing surfactant content enhances emulsion stability. At a concentration of 0.1%, no oil phase coalescing occurs over 180 days, and the droplet size increases by only 1.6 times the initial value. This enhanced stability is attributed to nanoparticles adsorbing irreversibly at the oil−water interface, reinforcing the emulsion's resistance to coalescence even under challenging conditions of inorganic salts and high temperatures.[41,44] Conversely, emulsion stability diminishes significantly at surfactant concentrations of 0.5 and 1.0%. Emulsions with 1.0% C16E20 exhibit a higher ROF compared to those with 0.001% C16E20, indicating that strongly hydrophilic nanoparticles may weaken the emulsion stability.

Further experiments explored the impact of the salinity on nanoparticle-stabilized emulsions. Pickering emulsions with 0.1% C16E20 were prepared by using saline solutions ranging from 1 to 4% NaCl. It is crucial to note that nanoparticles tend to flocculate in brine solutions with salinities exceeding 4%, making it impractical to prepare emulsions under these conditions. As observed, all the prepared emulsions exhibit zero ROF for at least 120 days. However, Figure 7 illustrates that the DRC curves of the Pickering emulsions are affected by the salinity. As observed, the DRC at different salinities is increased with the aging time, implying that oil coalescence occurs even when no oil is released. Besides, the DRC is increased with the salinity. For example, the DRC and 1−4% NaCl is 1.78, 2.03, 2.97 and 3.35, respectively after aging for 120 days. To explain the above result, the contact angle was measured at different salinity. It is

https://doi.org/10.1021/acsomega.4c06834
ACS Omega 2024, 9, 48427−48437

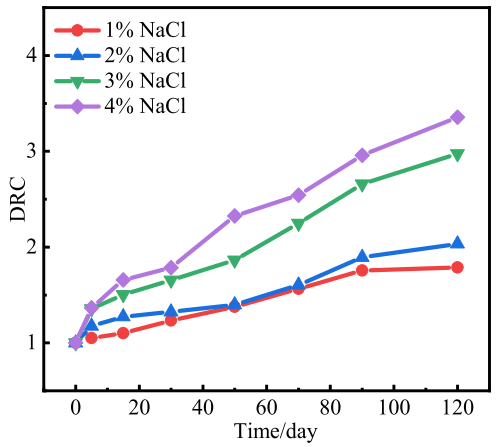

Figure 7. DRC of the emulsions with 0.001−1.0% C16E20 and 1.0% SiO_2 nanoparticles aging at 80 °C.

found that the contact angle gradually decreased from 78 to 47°, with the NaCl concentration ranging from 1 to 4%. It indicates that the added salt may compress the diffused double layer of the surfactant and the nanoparticles. Therefore, the efficiency of in situ modification is weakened. Overall, the results presented above indicate that the stability of these Pickering emulsions remains consistent across this salinity range. In conclusion, Pickering emulsions are adaptable to salinities below 4%, which adequately meet the requirements for chemical flooding applications at the current stage.

The viscosity of the emulsions is predominantly determined by the viscosity of its continuous phase and the concentration of the dispersed phase. When the concentration of the dispersed phase is low, the emulsions are considered to be diluted, meaning that the droplets within the emulsions are isolated from each other. Diluted emulsions typically exhibit Newtonian fluid behavior, where the viscosity remains constant, regardless of the shear rate. This behavior is described by Einstein's law:

$$\eta(\varphi) = \eta_0(1 + 2.5\varphi) \tag{4}$$

where η is the viscosity of emulsion, mPa·s. η_0 is the viscosity of the continuous phase, mPa·s. φ is the volume fraction of the dispersed phase.

Figure 8 illustrates the rheological behavior of Pickering emulsions containing varying concentrations of C16E20. At a low concentration of 0.001% C16E20, the emulsions demonstrate typical characteristics of a diluted emulsion, maintaining a nearly constant viscosity of 2 mPa·s across shear rates ranging from 1 to 100 s^{-1}, slightly higher than predicted by Einstein's law. As the concentration of C16E20 increases, the viscosity of the emulsion markedly rises, displaying non-Newtonian fluid behavior where viscosity decreases with the increasing shear rate. For instance, at 0.05% C16E20, the viscosity ranges from 180 mPa·s at 1 s^{-1} to 10 mPa·s at 100 s^{-1}. Emulsions containing 0.1% C16E20 exhibited peak viscosity. However, higher concentrations of C16E20 lead to reduced nanoparticle adsorption at the interface, resulting in a gradual decrease in emulsion viscosity with surfactant content. Furthermore, emulsions containing 1.0% C16E20 demonstrate higher viscosity than those with 0.5% C16E20 at low shear rates, while their viscosities converge at high shear rates.

Based on previous studies of nanoparticle-stabilized emulsions, the role of nanoparticles dictates their microstructure, thereby influencing their macroscopic properties. Microstructural observations were conducted using CLSM and cryo-SEM. Specifically, the fluorescent dye Rhodamine B was employed to label SiO_2 nanoparticles in CLSM, leveraging its positive charge for electrostatic interaction and detection. Figure 9 illustrates the microstructures of Pickering emulsions prepared at C16E20 concentrations of 0.01, 0.1, and 1.0%, representing systems with varying stability. For the emulsions with 0.01% C16E20, CLSM reveals red fluorescence signals at both the oil/water interface and within the continuous phase. Cryo-SEM images depict tightly stacked oil droplets that are isolated from each other, with slight surface roughness indicating adsorbed nanoparticles. However, nanoparticle distribution on droplet surfaces is nonuniform, with some dispersed in the continuous phases. In contrast, the emulsions with 0.1% C16E20 show strong fluorescence at the oil−water interface and throughout the continuous phase in CLSM, indicating extensive nanoparticles adsorption. Cryo-SEM images depict tightly stacked droplets bridged by a complex network structure, and rough surfaces confirm uniform nanoparticles adsorption. This adsorption configuration, characterized by high desorption energy, confers significant antiaggregation stability to Pickering emulsions, with excess nanoparticles forming a three-dimensional network. This microscopic structure enhances the emulsion's mechanical properties, i.e., highest viscosity. Conversely, in the emulsions with 1.0% C16E20, CLSM reveals minimal nanoparticle distribution at the oil−water interface, suggesting double-layer surfactant adsorption on nanoparticles, rendering them strongly hydrophilic. Cryo-SEM images show smooth droplet surfaces and bridging structures between droplets, likely due to surfactant association. This high surfactant content impedes nanoparticle adsorption at the interface, resembling conventional surfactant-stabilized emulsions rather than Pickering emulsions. In summary, nanoparticle-stabilized emulsions exhibit varying microstructures and stability, depending on surfactant concentration. Optimal stabilization and rheology occur at intermediate C16E20 concentrations where nanoparticles adsorb uniformly at the oil−water interface, forming a robust bridge-like structure.

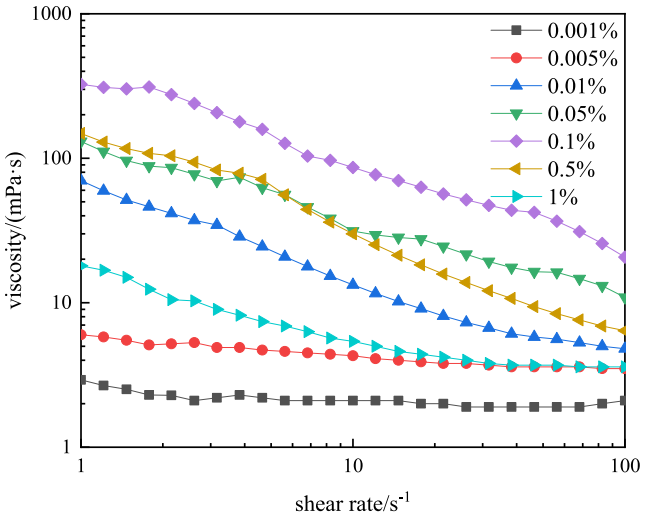

Figure 8. Viscosity curves versus shear rate of the Pickering emulsions with 0.001% C16E20 and 1.0% nanoparticles.

3.3. EOR Properties of Pickering Emulsions. To illustrate the permeation characteristics of different emulsion systems in porous media, we prepared four types of emulsions. The oil phase constituted 20% of the total volume, and the water phase

https://doi.org/10.1021/acsomega.4c06834
ACS Omega 2024, 9, 48427−48437

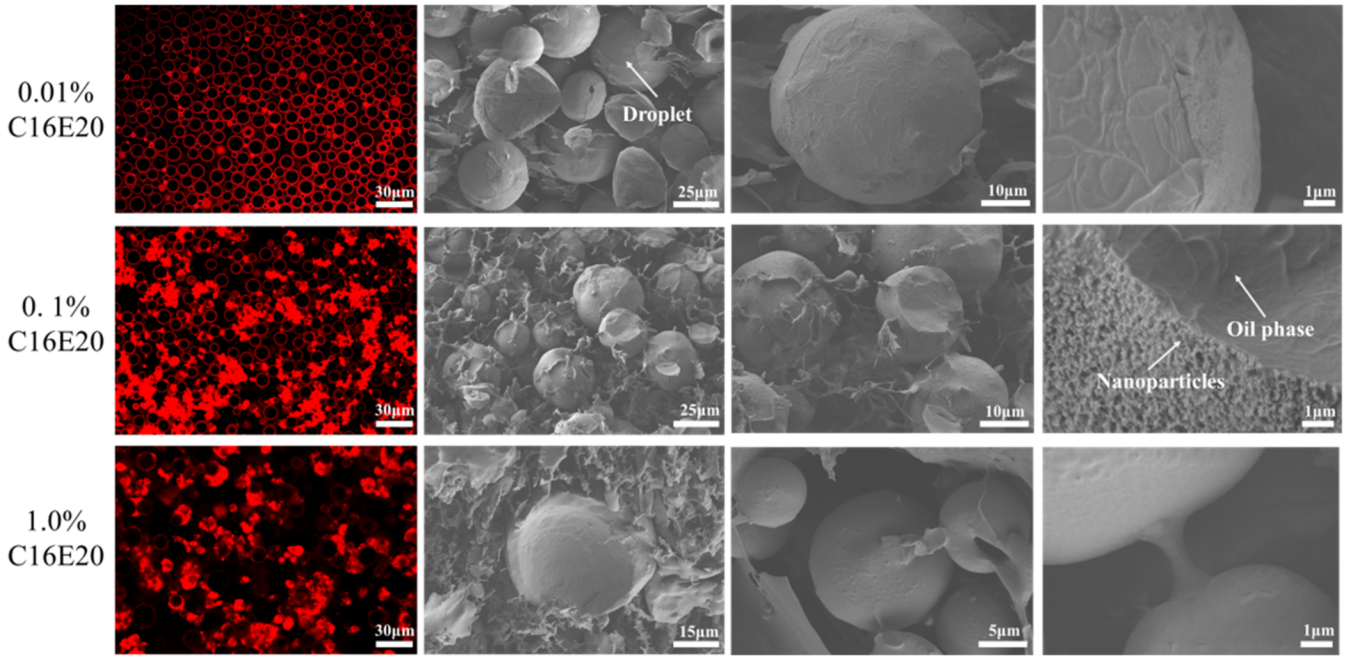

Figure 9. CLSM and cryo-SEM images of the Pickering emulsions with 1.0% nanoparticles and different C16E20 concentrations.

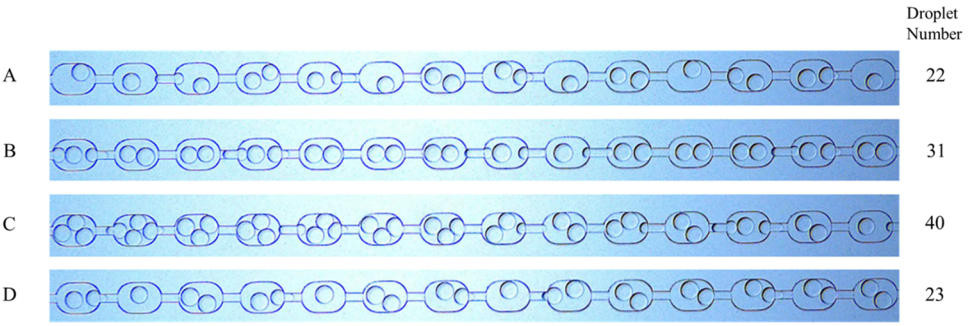

Figure 10. Image of different emulsion systems flowing in the microfluidics model at 104.15 $\mu m \cdot s^{-1}$.

was composed as follows: (a) 1.0% C16E20, (b) 0.01% C16E20 and 1.0% SiO_2 nanoparticles, (c) 0.1% C16E20 and 1.0% SiO_2 nanoparticles, and (d) 1.0% C16E20 and 1.0% SiO_2 nanoparticles. In addition, the droplet sizes of all the emulsions are 150 μm for comparison. When the droplets flow steadily through the pore throats, the number of droplets in the model reaches equilibrium. As shown in Figure 10, at a flow rate of 104.15 $\mu m \cdot s^{-1}$, the conventional emulsions (A and D) stabilized with C16E20 had 22 and 23 droplets, respectively. In contrast, the Pickering emulsions (B and C) exhibited greater retention at the pore throats, with 31 and 40 droplets, respectively, leading to a higher flow resistance.

Further experiments revealed that the differences in permeation characteristics caused by the composition of emulsions diminish as the flow rate increases. Figure 11 illustrates the number of droplets in the model at flow rates of 104.15, 208.30, and 416.60 $\mu m \cdot s^{-1}$. At a flow rate of 104.15 $\mu m \cdot s^{-1}$, significant differences in the number of droplets are observed. At 208.30 $\mu m \cdot s^{-1}$, the number of droplets in systems A and D remained almost unchanged, while the number of droplets in systems B and C decreased significantly. When the flow rate increased to 416.60 $\mu m \cdot s^{-1}$, the number of droplets in all systems decreased to around 15. These results suggest that high flow rates overcome the additional permeation resistance

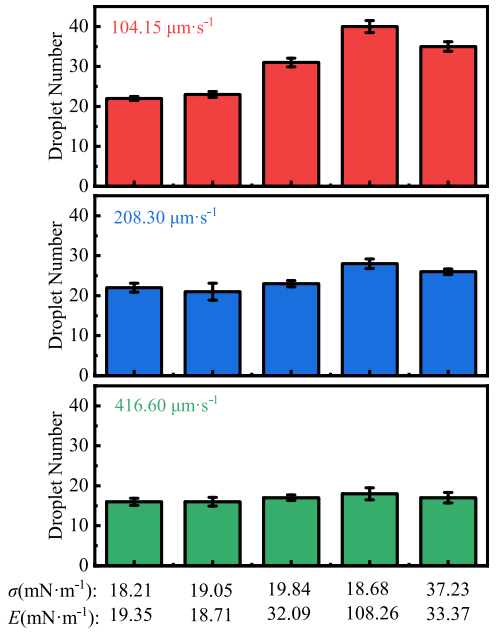

Figure 11. Droplet numbers of emulsions at flow rates of 104.15, 208.30, and 416.60 $\mu m \cdot s^{-1}$.

https://doi.org/10.1021/acsomega.4c06834
ACS Omega 2024, 9, 48427−48437

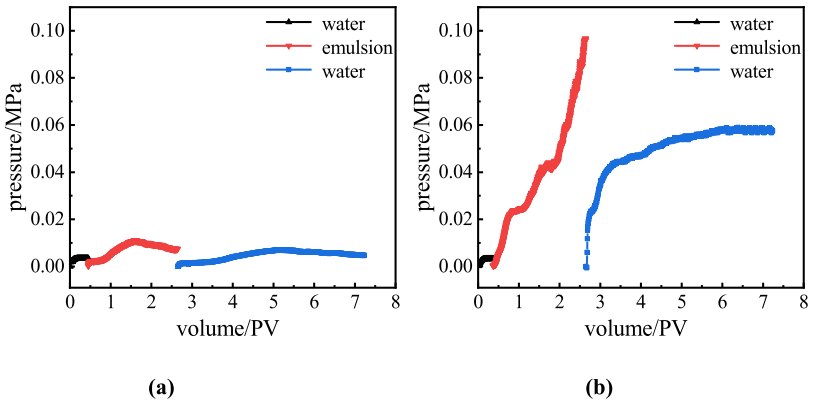

Figure 12. Injection pressure of the sand pack experiments for (a) conventional emulsions and (b) Pickering emulsions.

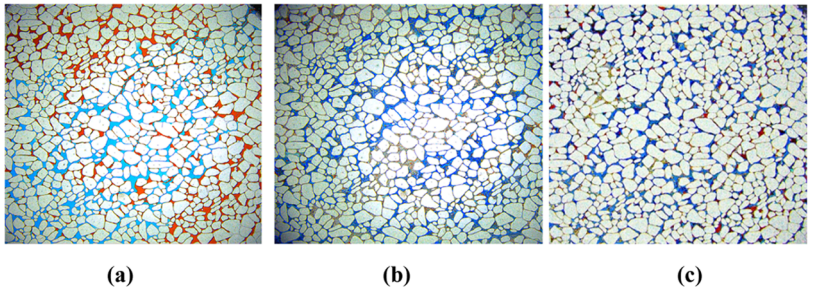

Figure 13. Images of the model after (a) waterflooding, (b) second waterflooding of the conventional emulsions, and (c) second waterflooding of the Pickering emulsions

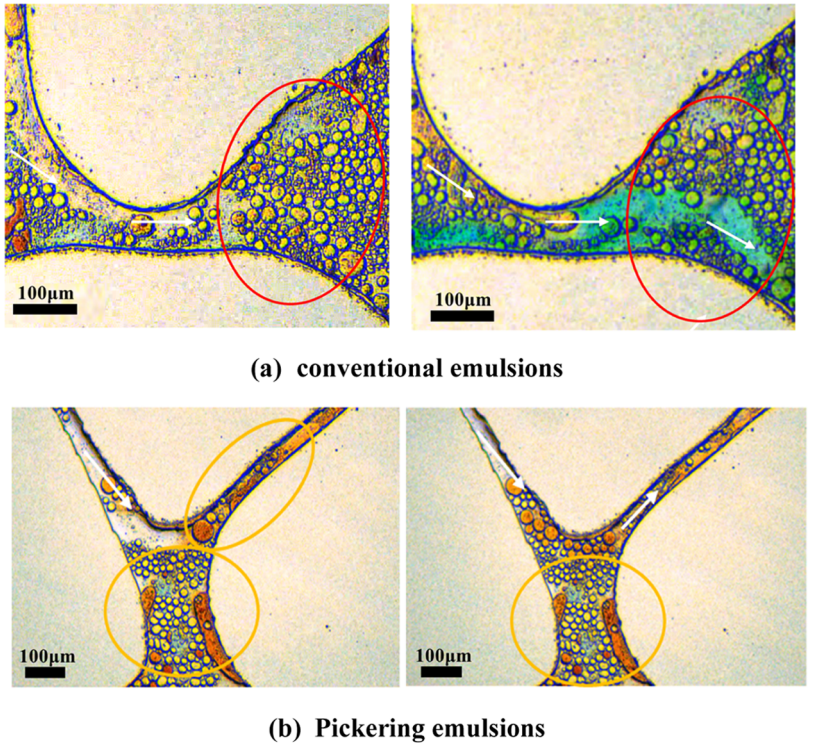

Figure 14. Microscopic images of the plug property for large pores of (a) conventional emulsions and (b) Pickering emulsions.

provided by the microstructure of the Pickering emulsions. Therefore, the application of Pickering emulsions requires low flow rates to fully demonstrate their advantages.

Figure 12 presents the injection pressure curves for conventional emulsions (system A) and Pickering emulsions (system C). To ensure optimal injection performance, both emulsions were diluted 4-fold, resulting in a 5% oil phase volume fraction. The sand pack models used have permeabilities of approximately 1000 mD, with an equilibrium pressure difference of 0.0033 MPa during water injection. During the injection of

https://doi.org/10.1021/acsomega.4c06834
ACS Omega 2024, 9, 48427−48437

conventional emulsions, the pressure initially increases and then decreases. At an injection volume of 2 pore volumes (PV), the pressure reaches 0.0074 MPa, resulting in a resistance factor of 2.24. In the subsequent water injection stage, the pressure equilibrates at 0.0046 MPa, with a residual resistance factor of 1.39. This indicates that conventional emulsions flow well through the sand packs but provide weaker conformance control. In contrast, the injection process of Pickering emulsions shows a sharp increase in the pressure. At an injection volume of 2 PV, the pressure reaches 0.098 MPa, resulting in a resistance factor of 29.70. During the subsequent water injection stage, the equilibrium pressure difference is 0.058 MPa, and the residual resistance factor is 17.6. These results suggest that Pickering emulsions exhibit significantly higher conformance control properties compared with conventional emulsions.

Oil displacement experiments were conducted to demonstrate the EOR properties of the emulsions. The typical oil displacement process includes four steps: (a) saturating the porous medium of the model with simulated oil, (b) injecting water until the water content of the produced liquid reaches 98%, known as waterflooding, (c) injecting about 0.3 pore volumes (PV) of chemical agents, and (d) injecting water again until the water content reaches 98%, known as the second waterflooding. The simulated oil and injected water were dyed red and blue, respectively. Figure 13a shows the oil−water distribution after waterflooding, revealing a water channel connecting the inlet (bottom left) and the outlet (top right) diagonally. During waterflooding, about 46−48% of the simulated oil is displaced. However, oil-rich zones that were not swept by the injected water remain beside the water channel, and isolated oil is trapped within the water channel. Emulsions have been used as EOR agents due to their conformance control properties. As the droplets of emulsions pass through the porous medium, the Jamin effect may create additional differential pressure if the droplets match the size of the pore throats. Consequently, the injected water bypasses the predominant pathways and accesses unswept oil-rich zones. Figure 13b,c displays the oil−water distribution after the second waterflooding, following the injection of conventional emulsions (system A) and Pickering emulsions (system C), respectively. The distribution of dyed water indicates that Pickering emulsions exhibit superior conformance control properties compared to conventional emulsions. As a result, approximately 12% of simulated oil is recovered using conventional emulsions, while about 20% is recovered with Pickering emulsions.

To illustrate the mechanism of the disparity in EOR efficiencies between these two emulsions, Microscopic details are displayed in Figure 14. According to the Jamin effect, the size of the droplet should be larger than the throat, so that the droplet is deformed when passing through the throat and provides additional pressure. In this case, conventional emulsions are not able to plug pores larger than them. As shown in Figure 14a, Droplets of conventional emulsions tend to migrate into and retain within larger pores. Although the droplets accumulate, the interaction between them is weak, allowing the large pores filled with emulsions to remain as predominant pathways for injected water. Referring to the Pickering emulsions, the modified nanoparticles can absorb on the oil−water interface and form a complex network. As shown in Figure 14b, the bridge structure is robust enough to resist the flow of injected water. Subsequently, the water flows into smaller pores and displaces the trapped and unswept oil. As a result, both the macroscopic and the microscopic sweep efficiency are improved since the Pickering emulsions can plug much larger pores, leading to greater oil recovery.

4. CONCLUSIONS

(1) To prepare Pickering emulsions, the hydrophilic SiO_2 nanoparticles should be modified by surfactant. In this work, optimal hydrophilic−hydrophobic balance is achieved by mixing the surfactant C16E20 and nanoparticles in ratios of 0.1 and 1.0%. The resulting emulsions are stable for at least 180 days in salinities below 4% NaCl at 80 °C, which meet the demand of EOR at harsh reservoirs. Besides, these emulsions also exhibit much higher viscosity than conventional emulsions.

(2) Pickering emulsions offer superior conformance control properties compared to conventional emulsions. Microfluidic and flow experiments reveal that Pickering emulsions tend to be retained in pore throats and require a higher additional injection pressure. Additionally, oil displacement tests in a 2D model demonstrate that Pickering emulsions can effectively block much larger than the droplet size and improve oil recovery by approximately 20%, compared to a 12% increase with conventional emulsions.

■ ASSOCIATED CONTENT

Data Availability Statement

The data that support the findings of this study are openly available in this manuscript.

■ AUTHOR INFORMATION

Corresponding Author

Guicai Zhang − *School of Petroleum Engineering, China University of Petroleum (East China), Qingdao, Shandong 266580, China;* orcid.org/0000-0001-9623-2583; Email: zhanggc@upc.edu.cn

Authors

Liu Yang − *School of Petroleum Engineering, China University of Petroleum (East China), Qingdao, Shandong 266580, China*

Jijiang Ge − *School of Petroleum Engineering, China University of Petroleum (East China), Qingdao, Shandong 266580, China*

Hao Wu − *Sinopec Shengli Oilfield Petroleum Engineering Technology Research Institute, Dongying, Shandong 257091, China*

Xiaqing Li − *Sinopec Shengli Oilfield Petroleum Engineering Technology Research Institute, Dongying, Shandong 257091, China*

Jianda Li − *Sinopec Shengli Oilfield Petroleum Engineering Technology Research Institute, Dongying, Shandong 257091, China*

Complete contact information is available at: https://pubs.acs.org/10.1021/acsomega.4c06834

Author Contributions

L.Y.: writing—original draft, J.G.: writing—review and editing, H.W.: investigation, X.L.: visualization, X.Z.: visualization, and G.Z.: conceptualization.

Notes

The authors declare no competing financial interest.

https://doi.org/10.1021/acsomega.4c06834
ACS Omega 2024, 9, 48427−48437

Ethical approval Ethical approval was not required for the study.

■ ACKNOWLEDGMENTS

This research did not receive any specific grant from funding agencies in the public, commercial, or not-for-profit sectors.

■ REFERENCES

(1) Daigle, H.; Griffith, N. In *Optimizing Nanoparticle-Stabilized Emulsion Behavior in Porous Media Through Electrostatic Interactions*, SPE Annual Technical Conference and Exhibition? SPE, 2018.
(2) Yu, L.; Ding, B.; Dong, M.; Jiang, Q. A new model of emulsion flow in porous media for conformance control. *Fuel* **2019**, *241*, 53−64.
(3) Koroleva, M.; Nagovitsina, T. Y.; Yurtov, Evgeny V. Nano-emulsions stabilized by non-ionic surfactants: stability and degradation mechanisms. *Phys. Chem. Chem. Phys.* **2018**, *20*, 10369−10377.
(4) Hirasaki, G. J.; Miller, A.; Puerto, M. Recent Advances in Surfactant EOR. *SPE J.* **2011**, *16* (04), 889−907.
(5) Malhotra, V.; Pal, R.; Alhassan, S. Catastrophic Phase Inversion of Emulsions Stabilized by Amphiphilic Nanoparticles. *J. Nanofluids* **2018**, *7* (1), 30−36.
(6) Griffith, Christopher.; Daigle, Hugh. Manipulation of Pickering emulsion rheology using hydrophilically modified silica nanoparticles in brine. *J. Colloid Interface Sci.* **2018**, *509*, 132−139.
(7) Salama, I. E.; Paul, A. Emulsions of fluorinated oils stabilised by fluorinated silica nanoparticles. *Colloids Surf., A* **2016**, *494*, 125−138.
(8) Mohammadkhani, S.; Shahverdi, H.; Esfahany, M. N. Impact of salinity and connate water on low salinity water injection in secondary and tertiary stages for enhanced oil recovery in carbonate oil reservoirs. *J. Geophys. Eng.* **2018**, *15* (4), 1242−1254.
(9) Georges Lwisa, E.; Abdulkhalek, A. R. Enhanced oil recovery by nitrogen and carbon dioxide injection followed by low salinity water flooding for tight carbonate reservoir: experimental approach. *Mater. Sci. Eng.* **2018**, No. 012009.
(10) Park, J. B.; Uhlmann, D. R. Recovery of deformed polymers. III. Thermal properties. *J. Appl. Phys.* **1973**, *44* (1), 201−206.
(11) Alquriaishi, A. A.; Shokir, E. M. El-M. Experimental Investigation of Miscible CO_2 Flooding. *Pet. Sci. Technol.* **2011**, *29* (19), 2005−2016.
(12) Sheng, J. J.; Leonhardt, B.; Azri, N. Status of Polymer-Flooding Technology. *Journal of Canadian Petroleum Technology* **2015**, *54* (02), 116−126.
(13) Zhu, Y. Y.; Luo, W. L.; Jian, G. Q.; Wang, C. A.; Hou, Q. F.; Niu, J. L. Development and Performance of Water Soluble Salt-Resistant Polymers for Chemical Flooding. *Adv. Mater. Res.* **2015**, 476−478.
(14) Delamaide, E.; Bazin, B.; Rousseau, D.; Degre, G. In *Chemical EOR for Heavy Oil: The Canadian Experience*, SPE EOR Conference at Oil and Gas West Asia, SPE: 2014.
(15) Zhong, X.; Wang, Y.; Pu, H.; Li, W.; Yin, S.; Ling, K. In *Commercial Implementation of Chemical Flooding in Daqing Oilfield, China, and Its Future*, SPE EOR Conference at Oil and Gas West Asia; SPE, 2018.
(16) Park, S.; Lee, E. S.; Sulaiman, W. R. W. Adsorption behaviors of surfactants for chemical flooding in enhanced oil recovery. *J. Ind. Eng. Chem.* **2015**, *21*, 1239−1245.
(17) Li, X.; Liu, Y.; Li, S.; Tang, J. Dissipative particle dynamics simulation of wettability alternation phenomena in the chemical flooding process. *Acta Mech. Sin.* **2009**, *25*, 583−587.
(18) Al-Asadi, A.; Rodil, E.; Soto, A. Nanoparticles in Chemical EOR: A Review on Flooding Tests. *Nanomaterials* **2022**, *12* (23), 4142.
(19) Li, K.; Ovsepian, M.; Xie, W.; Varfolomeev, M. A.; Luo, Q.; Yuan, C. Emulsions for enhanced oil recovery: Progress and prospect. *J. Mol. Liq.* **2024**, *393*, No. 123658.
(20) Maurya, N. K.; Mandal, A. Investigation of synergistic effect of nanoparticle and surfactant in macro emulsion based EOR application in oil reservoirs. *Chem. Eng. Res. Des.* **2018**, *132*, 370−384.
(21) Wang, T.; Wang, L.; Meng, X.; Chen, Y.; Song, W.; Yuan, C. Key parameters and dominant EOR mechanism of CO_2 miscible flooding applied in low-permeability oil reservoirs. *Geoenergy Sci. Eng.* **2023**, *225*, No. 211724.
(22) Guillen, V. R.; Carvalho, M. S.; Alvarado, V. Pore Scale and Macroscopic Displacement Mechanisms in Emulsion Flooding. *Transp. Porous Media* **2012**, *94* (1), 197−206.
(23) Guillen, V. R.; Romero, M. I.; Carvalho, M. d. S.; Alvarado, V. Capillary-driven mobility control in macro emulsion flow in porous media. *Int. J. Multiphase Flow* **2012**, *43*, 62−65.
(24) Kumar, N.; Gaur, T.; Mandal, A. Characterization of SPN Pickering emulsions for application in enhanced oil recovery. *J. Ind. Eng. Chem.* **2017**, *54*, 304−315.
(25) Shakir, H. A.; Abdulhameed, R. F.; Hilal, H. A. A.; Alfarge, D.; Aljarah, A. M. Factors impacting the performance of polymer-based EOR in oil reservoirs. *Chem. Pap.* **2023**, *77* (9), 4859−4875.
(26) Jain, S.; Pachisia, H.; Sharma, A.; Patel, S.; Patel, S.; Ragunathan, B. A systematic review—Chemical EOR using surfactants and polymers. *Mater. Today: Proc.* **2022**, *62*, 7220−7223.
(27) Jia, H.; Wang, D.; Wang, Q.; Dai, J.; Wang, Q.; Wen, S.; Wang, Z.; Wang, B.; Jiang, X.; Li, X.; Lv, K. The synthesis of novel amphiphilic GOJS-Cn nanoparticles and their further application in stabilizing pickering emulsion and enhancing oil recovery. *J. Pet. Sci. Eng.* **2022**, *214*, No. 110537.
(28) AfzaliTabar, M.; Alaei, M.; Bazmi, M.; Ranjineh Khojasteh, R.; Koolivand Salooki, M.; Motiee, F.; Rashidi, A. Facile and economical preparation method of nanoporous graphene/silica nanohybrid and evaluation of its Pickering emulsion properties for Chemical Enhanced oil Recovery (C-EOR). *Fuel* **2017**, *206*, 453−466.
(29) Horozov, T. S.; Binks, B. P.; Aveyard, R.; Clint, J. H. Effect of particle hydrophobicity on the formation and collapse of fumed silica particle monolayers at the oil-water interface. *Colloids Surf., A* **2006**, *282*−*283*, 377−386.
(30) Fouconnier, B.; Román-Guerrero, A.; Vernon-Carter, E. J. Effect of [CTAB]-[SiO_2] ratio on the formation and stability of hexadecane/water emulsions in the presence of NaCl. *Colloids Surf., A* **2012**, *400*, 10−17.
(31) Dong, J.; Worthen, A. J.; Foster, L. M.; Chen, Y.; Cornell, K. A.; Bryant, S. L.; Truskett, T. M.; Bielawski, C. W.; Johnston, K. P. Modified montmorillonite clay microparticles for stable oil-in-seawater emulsions. *ACS Appl. Mater. Interfaces* **2014**, *6* (14), 11502−11513.
(32) Mahboob, A.; Sultan, A. S.; Adewunmi, A. A.; Kamal, M. S. In *Conformance Control in Harsh Reservoir Conditions Using a Novel Pickering Emulsion*, SPE Gas & Oil Technology Showcase and Conference; SPE, 2023.
(33) Cui, Y.; Threlfall, M.; van Duijneveldt, J. S. Optimizing organoclay stabilized Pickering emulsions. *J. Colloid Interface Sci.* **2011**, *356* (2), 665−671.
(34) Wang, J.; Sun, Y.; Yu, M.; Lu, X.; Komarneni, S.; Yang, C. Emulsions stabilized by highly hydrophilic TiO_2 nanoparticles via van der Waals attraction. *J. Colloid Interface Sci.* **2021**, *589*, 378−387.
(35) Binks, B. P.; Rodrigues, J. A.; Frith, W. J. Synergistic interaction in emulsions stabilized by a mixture of silica nanoparticles and cationic surfactant. *Langmuir* **2007**, *23* (7), 3626−3636.
(36) Stehl, D.; Hohl, L.; Schmidt, M.; Hübner, J.; Lehmann, M.; Kraume, M.; Schomäcker, R.; von Klitzing, R. Characteristics of Stable Pickering Emulsions under Process Conditions. *Chem. Ing. Tech.* **2016**, *88* (11), 1806−1814.
(37) Li, X.-L.; Liu, W.; Xu, B.; Bao, Z. Simple method for fabrication of high internal phase emulsions solely using novel pea protein isolate nanoparticles: Stability of ionic strength and temperature. *Food Chem.* **2022**, *370*, No. 130899.
(38) He, Y.; Wu, F.; Sun, X.; Li, R.; Guo, Y.; Li, C.; Zhang, Lu.; Xing, F.; Wang, Wei.; Gao, J. Factors that affect Pickering emulsions stabilized by graphene oxide. *ACS Appl. Mater. Interfaces* **2013**, *5* (11), 4843−4855.
(39) Zargartalebi, M.; Kharrat, R.; Barati, N. Enhancement of surfactant flooding performance by the use of silica nanoparticles. *Fuel* **2015**, *143*, 21−27.
(40) Alomair, O. A.; Matar, K.; Hamed Alsaeed, Y. Experimental study of enhanced-heavy-oil recovery in Berea sandstone cores by use of

https://doi.org/10.1021/acsomega.4c06834
ACS Omega 2024, 9, 48427−48437

nanofluids applications. *SPE Reservoir Eval. Eng.* **2015**, *18* (03), 387−399.
(41) Binks, B. P.; Rodrigues, J. A. Enhanced Stabilization of Emulsions Due to Surfactant-Induced Nanoparticle Flocculation. *Langmuir* **2007**, *23*, 7436−7439.
(42) Binks, B. P.; Whitby, C. P. Nanoparticle silica-stabilised oil-in-water emulsions: improving emulsion stability. *Colloids Surf., A* **2005**, *253* (1−3), 105−115.
(43) Binks, B. P.; Desforges, A.; Duff, D. G. Synergistic Stabilization of Emulsions by a Mixture of Surface-Active Nanoparticles and Surfactant. *Langmuir* **2007**, *23*, 1098−1106.
(44) Xu, M.; Jiang, J.; Pei, X.; Song, B.; Cui, Z.; Binks, B. P. Angewandte Chemie. Novel Oil-in-Water Emulsions Stabilised by Ionic Surfactant and Similarly Charged Nanoparticles at Very Low Concentrations. *Angew. Chem., Int. Ed.* **2018**, 7738−7742.
(45) Xu, M.; Xu, L.; Lin, Q.; Pei, X.; Jiang, J.; Zhu, H.; Cui, Z.; Binks, B. P. Switchable Oil-in-Water Emulsions Stabilized by Like-Charged Surfactants and Particles at Very Low Concentrations. *Langmuir* **2019**, *35*, 4058−4067.
(46) Midmore, B. R. Preparation of a novel silica-stabilized oil/water emulsion. *Colloids Surf., A* **1998**, *132* (2−3), 257−265.
(47) Vignati, E.; Piazza, R.; Lockhart, T. P. Pickering Emulsions: Interfacial Tension, Colloidal Layer Morphology, and Trapped-Particle Motion. *Langmuir* **2003**, *19*, 6650−6656.
(48) Maurya, N. K.; Kushwaha, P.; Mandal, A. Studies on interfacial and rheological properties of water soluble polymer grafted nanoparticle for application in enhanced oil recovery. *J. Taiwan Inst. Chem. Eng.* **2017**, *70*, 319−330.
(49) Kostakis, T.; Ettelaie, R.; Murray, B. S. Effect of High Salt Concentrations on the Stabilization of Bubbles by Silica Particles. *Langmuir* **2006**, *22* (3), 1273−1280.
(50) Derkach, S. R. Rheology of emulsions. *Adv. Colloid Interface Sci.* **2009**, *151* (1−2), 1−23.
(51) Chen, J.; Vogel, R.; Werner, S. R. L.; Heinrich, G.; Clausse, D.; Dutschk, V. Influence of the particle type on the rheological behavior of Pickering emulsions. *Colloids Surf., A* **2011**, *382* (1−3), 238−245.

https://doi.org/10.1021/acsomega.4c06834
ACS Omega 2024, 9, 48427−48437